TÜBİTAK

Turk J Elec Eng & Comp Sci, Vol.20, No.3, 2012, © TÜBİTAK
doi:10.3906/elk-1011-955

A simulator based on an energy-efficient GPR algorithm modified for the scanning of all types of regions

Levent SEYFİ*, Ercan YALDIZ
Department of Electrical and Electronics Engineering, Faculty of Engineering and Architecture, Selçuk University, 42031 Konya-TURKEY
e-mail: leventseyfi@selcuk.edu.tr, eyaldiz@selcuk.edu.tr

Received: 23.11.2010

Abstract

An improved simulator is presented for the simulation of an energy-efficient ground-penetrating radar (GPR) using the 2D finite-difference time-domain method in the MATLAB environment. This simulator is novel in that it improves on previous work that did not involve scanning a buried object or the intermittent sublayer beneath the ground using an energy-efficient algorithm. The present simulator examines the scanned region and automatically chooses either a common algorithm or an energy-efficient algorithm, depending on the region. The simulator provides the possibility of using an energy-efficient GPR without the need for the operator to determine the suitability of the scanned region. Three different models are defined to confirm the validity of the simulator. These models separately include an inclined sublayer, a rough sublayer, and a buried object. The obtained results show that the energy-efficient GPR can be used in all types of regions.

Key Words: *Energy saving, finite-difference time-domain, ground-penetrating radar, numerical computing*

1. Introduction

Ground-penetrating radar (GPR) has a wide area of usage, such as determining the thickness and structure of glaciers, locating ice in permafrost, finding sewer lines and buried cables, measuring the thickness of sea ice, profiling the bottoms of lakes and rivers, examining the subsurface of the moon, detecting buried containerized hazardous waste, and measuring scouring around bridge foundations [1].

Investigation of subsurfaces with GPR enables the user to get information about the medium without much effort. GPR, among other nondestructive detection techniques, has been rising in popularity owing to its high resolution and its abilities of wide sensing. GPR systems comprise a transmitter, receiver, data storage, control unit, and data display, as shown in Figure 1. The transmitter sends very short pulses of radio frequency (RF) energy. The transmitted pulse is radiated downward by the radar antenna into the subsurface. A portion of the RF energy is reflected wherever there is a change or discontinuity in the electrical properties of the

*Corresponding author: Department of Electrical and Electronics Engineering, Faculty of Engineering and Architecture, Selçuk University, 42031 Konya-TURKEY

medium. The rest of the energy propagates through the interface. The amplitudes of the signals reflected from and passed through the boundary depend on the difference of the electrical properties between the regions and the roughness of the interface. RF reflections or target echoes are obtained by receiving antenna and are processed for display, recording, and detection. The GPR composes the image data by receiving a reflection signal from different objects or layers in the host region [2-4]. The image data may be composed in 3 different forms, namely A-scans, B-scans, and C-scans. The A-scan is a stationary measurement from a specific position on the surface, presented in the form of a time-series signal. A set of A-scans constitutes a B-scan image, and a group of B-scan images forms a 3-dimensional C-scan data cube [5].

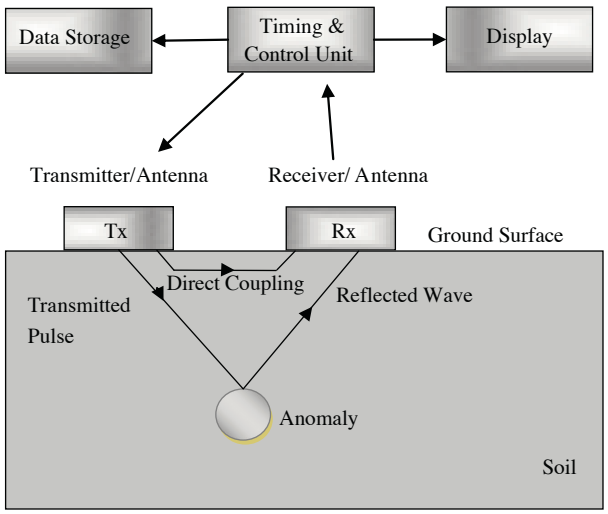

Figure 1. Principles of a GPR system.

Many methods can be used to numerically simulate GPR scanning, such as ray-based methods [6], frequency-domain methods [7], integral methods [8], pseudospectral methods [9], and the finite-difference time-domain (FDTD) method [10,11]. Because the FDTD approach is conceptually simple, accurate for arbitrarily complex models, and capable of accommodating realistic antenna designs and their features such as dispersion in electrical properties, it is the most common approach to be used at present [12-14].

In this paper, a 2D FDTD method was employed to develop a simulator in the MATLAB environment. A 2D method was chosen because it requires less computer memory and less time than 3D methods [15]. The transverse electric (TE) mode was used for the 2D FDTD approach. The simulator involves perfectly matched layer (PML) absorbing boundaries to avoid reflections from the edges of the modeling grid. Further information about PMLs can be found in [16,17].

Energy saving is of much importance for GPR, similar to other portable devices, since there is no electrical source in the field to be used with a GPR system. Thus, the system's battery must be carefully used as efficiently as possible. To run a GPR system efficiently, it is necessary to focus our attention on managing the transmitter power.

In our previous study, simulator software for saving transmitter energy in GPR systems was utilized [18]. It was found there that a GPR with an energy-efficient algorithm was suitable for considerable energy savings while detecting continual and smooth sublayers, such as profiling continuous pavement and the bottoms of lakes, but it did not provide the expected efficiency for detection of rough layers and intermittent targets, such as in

mine detection. This study aimed for improvement of the previous results. The proposed simulator allows use of the GPR with energy-saving properties for all applications, even if the application medium is not thoroughly suited for use of the energy-efficient GPR algorithm. The simulator makes it possible to both save energy while using the GPR in proper media and to use the GPR confidently in other media.

2. 2D FDTD method

FDTD is a well known time-domain method used for representing wave propagation. No variation is mentioned through third coordinates in 2D problems. Here, the third coordinate is selected as the z-axis. TE or transverse magnetic (TM) modes exist when reduction of 3D FDTD to 2D FDTD is carried out. In this study, a TE mode whose formulas are given below was employed.

$$\frac{\partial E_x}{\partial t} = \frac{1}{\varepsilon}\left(\frac{\partial H_z}{\partial y} - \sigma E_x\right) \tag{1a}$$

$$\frac{\partial E_y}{\partial t} = \frac{1}{\varepsilon}\left(\frac{\partial H_z}{\partial x} - \sigma E_y\right) \tag{1b}$$

$$\frac{\partial H_z}{\partial t} = \frac{1}{\mu}\left(\frac{\partial E_x}{\partial y} - \frac{\partial E_y}{\partial x} - \rho' H_z\right) \tag{1c}$$

More information about the FDTD technique can be found in [19].

3. Considered structural models

Three models are intentionally described to analyze situations that are both suitable and unsuitable for scanning with the energy-efficient GPR algorithm. Model 1, proposed in Figure 2, is considered to be more appropriate for scanning with the energy-efficient algorithm, and the other 2 models given in Figures 3 and 4 are respectively considered to be inappropriate for scanning with the energy-efficient algorithm.

As seen in Figure 2, the first model has an inclined sublayer, while the second model, in Figure 3, has a wavy and rough sublayer. The third model, in Figure 4, has a buried object. For all cases, the medium is assumed to be a vacuum having magnetic permeability (μ_o). The related relative dielectric permittivity (ε_r) and the electrical conductivities (σ) for the models are given in Figures 2-4, respectively.

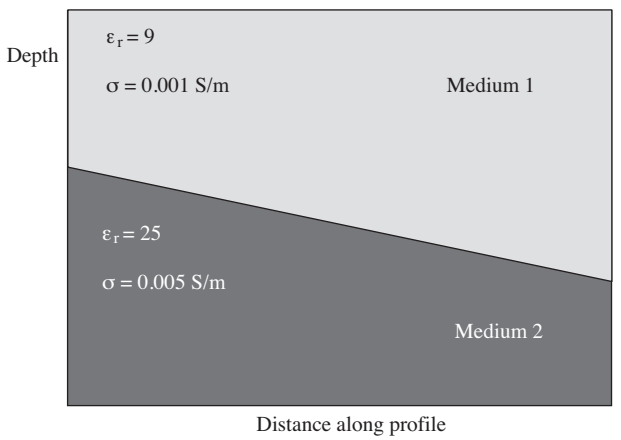

Figure 2. Layout of model 1, including an inclined sublayer.

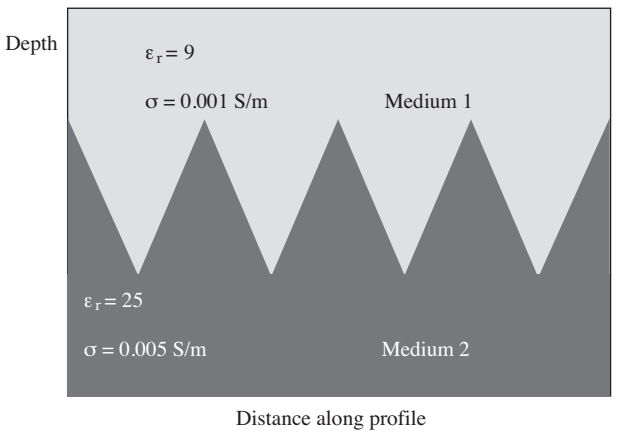

Figure 3. Layout of model 2, including a wavy and rough sublayer.

4. Developed simulator

The simulator developed in the MATLAB environment employs a new algorithm for 2D numerical computation for GPR scanning purposes. It can simulate 2D GPR scanning to obtain results related to the B-scan image data.

The flowchart of the proposed algorithm for the improved simulator is depicted in Figure 5. The algorithm includes both the common and the energy-efficient GPR algorithms [18]. The GPR scanning is performed at all steps in position (from b = 1 to b = last step). Until b = 10, the energy-efficient algorithm is utilized, and then the consumed energy is calculated to verify if there is any apparent saving of energy. If there is energy saving, the energy-efficient algorithm continues to be used, with the situation being examined at each space increment. However, if energy savings are not achieved, the simulator is automatically switched to the common algorithm, which is sustained until the last position step of the simulation. Eventually, the percentage of total energy saved is displayed and the obtained B-scan radar image is plotted.

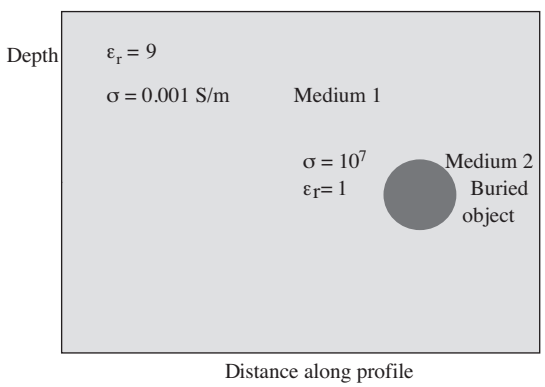

Figure 4. Layout of model 3, including a buried object.

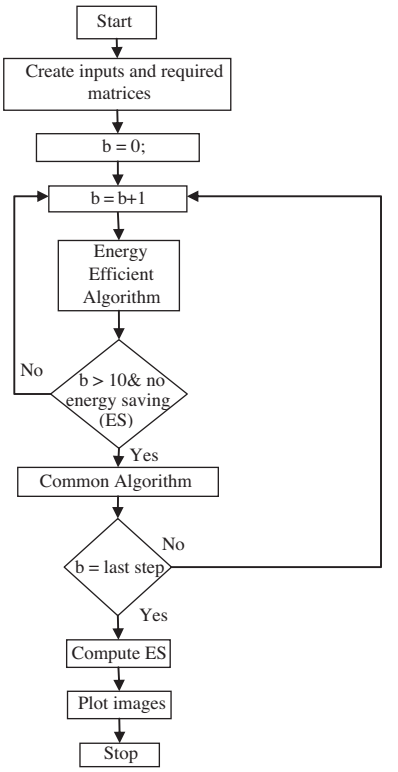

Figure 5. Flowchart of the proposed simulator.

5. Numerical results

Spatial increments in the x- and y-axes were considered to be equal to dx. A spatial increment (dx) and a temporal step (dt) were selected as 3 mm and 5 ps, respectively, for all models. The temporal step was computed to guarantee the stability condition with $dt = dx/(2 \cdot c)$, where c is the velocity of light in a vacuum. Eight-cell PML boundaries were employed to truncate the computation domain. The source was assumed to be the sine-modulated Gaussian pulse defined in Eq. (2) below. Selecting a sine-modulated Gaussian pulse as the

source makes detecting targets in the GPR results easier.

$$\text{Source } = A \cdot \sin\left(w\left(t - t_o\right)\right) \cdot e^{\left(-0.5 \cdot \left((t-t_o)/\tau\right)^2\right)} \tag{2}$$

Here, A, the amplitude of the signal, was selected as 410 in the common algorithm and as varying in the energy-efficient algorithm; w is the angular frequency $2\pi 10^8$ rad/s; t_o is 96 s; and time constant τ is 32.

B-scan image outputs from the simulator containing the proposed energy-efficient algorithm for 3 different models are given in Figures 6, 8, and 10, respectively. Results obtained from the common GPR algorithm for comparison with the results of the proposed simulator are illustrated in Figures 7, 9, and 11, respectively.

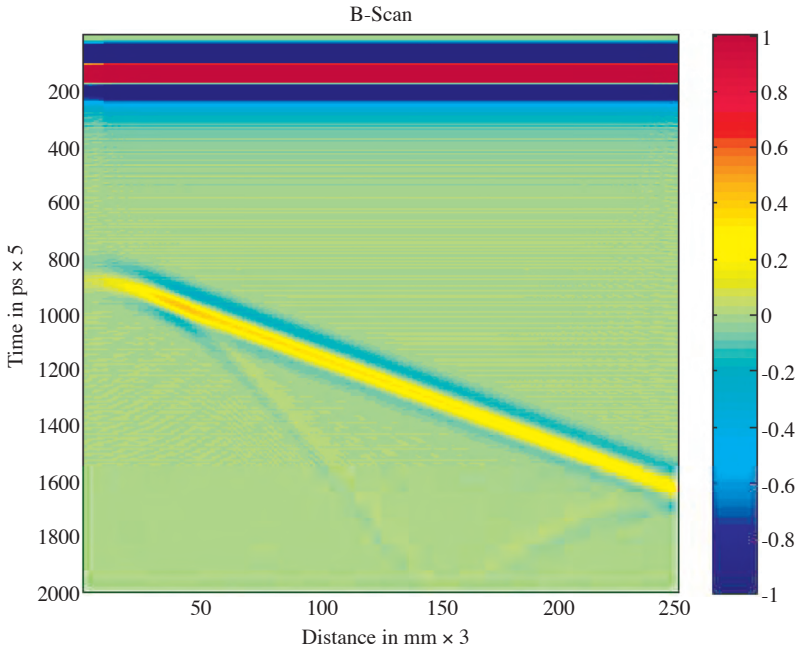

Figure 6. B-scan image obtained from model 1 using the proposed algorithm.

The image in Figure 6 was obtained from model 1, given in Figure 2, in which merely the energy-efficient algorithm was employed. It was shown in our previous study that model 1 was a suitable choice for proper use of the energy-efficient algorithm, giving energy savings of 22% [18]. The image in Figure 7 was obtained from model 1 using only the common GPR algorithm.

The image in Figure 8 was obtained from model 2, illustrated in Figure 3. In this case, both the energy-efficient algorithm and the common algorithm were employed. First, the energy-efficient algorithm was used; then the simulator determined that the common GPR algorithm was more convenient for this model and continued scanning with the common GPR algorithm. The image in Figure 9 was obtained from model 2 using only the common GPR algorithm.

The image in Figure 10 was obtained from model 3, shown in Figure 4. In the case of model 3, both the energy-efficient algorithm and the common algorithm were conveniently used. The simulator started with the energy-efficient algorithm, then determined that the common GPR algorithm was better for this model and continued scanning with the common GPR algorithm. The image seen in Figure 11 was obtained from model 3 by means of the common GPR algorithm only.

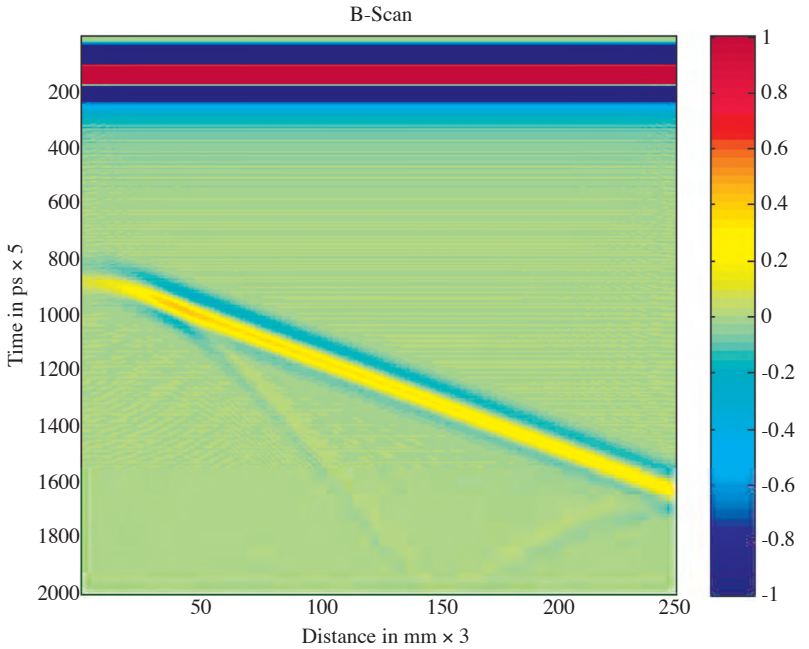

Figure 7. B-scan image obtained from model 1 using the common algorithm [18].

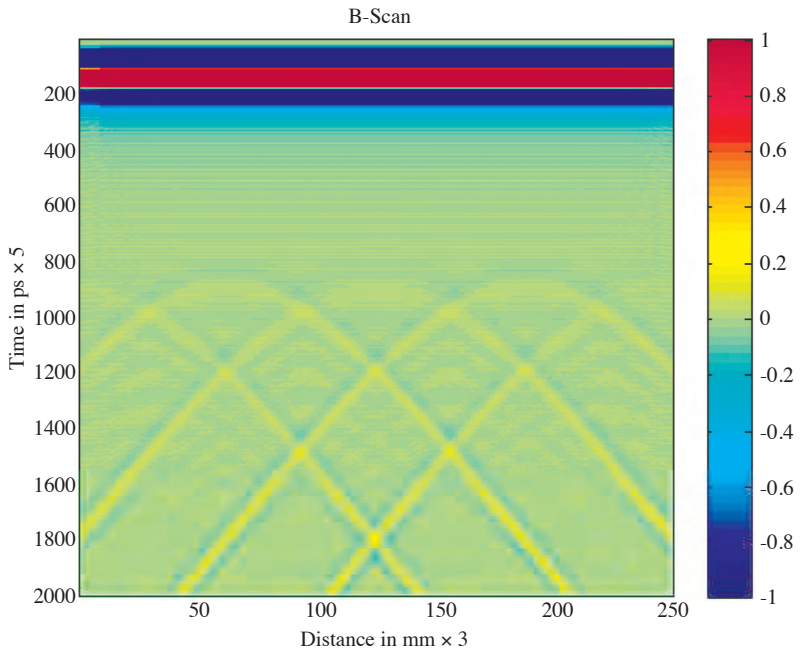

Figure 8. B-scan image obtained from model 2 using the proposed algorithm.

The vertical axis in B-scan images is a time scale, showing the time it takes for the GPR signal to travel through the medium and return to the antenna. If the velocity of the transmitted signal propagation can be calculated, this time scale may be converted into a depth scale by using the simple equation of velocity $\times$ time = depth. The horizontal scale represents the distance travelled along the profile.

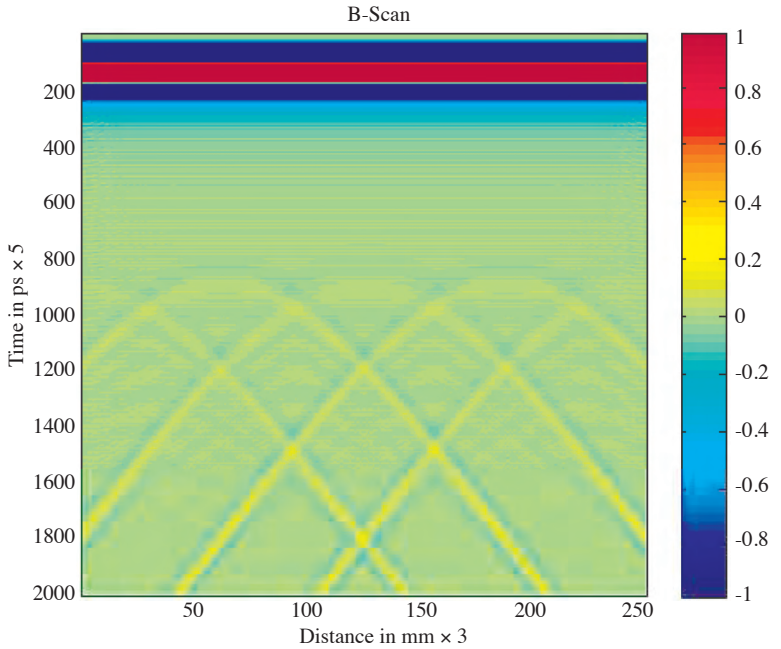

Figure 9. B-scan image obtained from model 2 using the common algorithm.

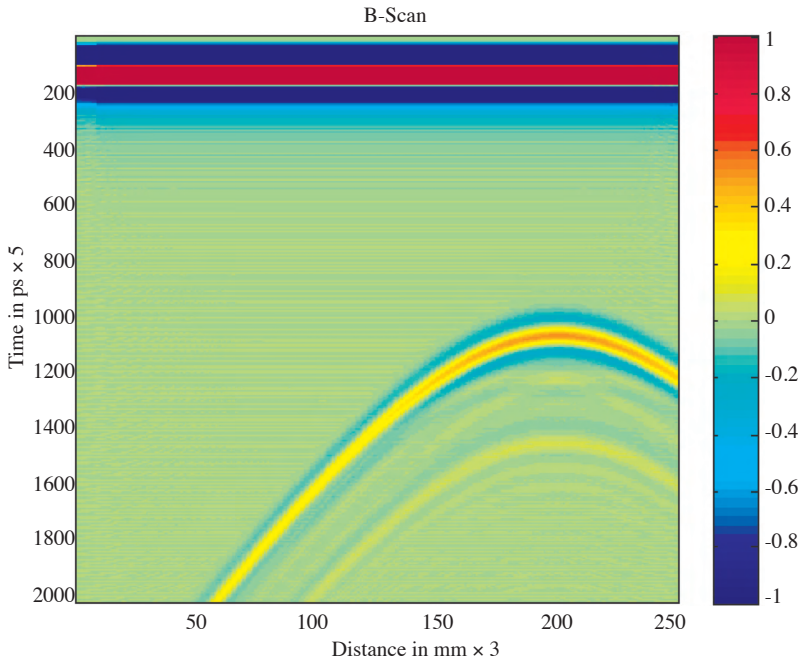

Figure 10. B-scan image obtained from model 3 using the proposed algorithm.

A longer time between the transmission and reception of a signal in a given homogeneous medium generally implies a greater distance to a given interface.

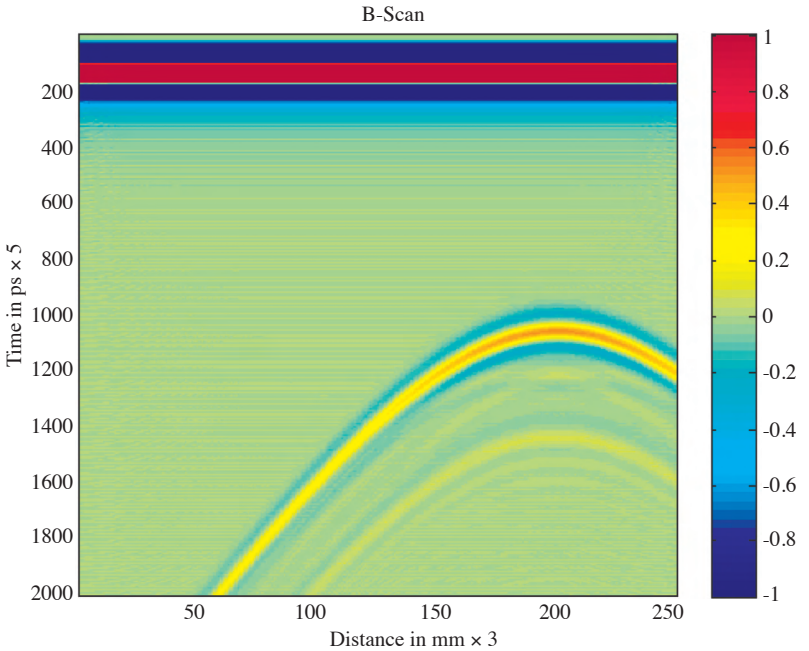

Figure 11. B-scan image obtained from model 3 using the common algorithm.

6. Conclusion

In our previous study, it was found that the energy-efficient GPR algorithm was suitable for considerable energy savings while detecting continual and smooth sublayers. However, this algorithm did not yield the expected results for rough layers and intermittent targets.

In this study, a new simulator was composed to use the energy-efficient GPR algorithm for scanning all types of regions. Since this simulator can automatically choose between the energy-efficient and common GPR algorithms during GPR scanning, it enables the user to take advantage of energy-efficient GPR without dependence on the type of region. Two different models that were not convenient for use of the energy-efficient algorithm were employed to prove the success of the new proposed simulator. As shown, the proposed algorithm presents very close results to those of the common algorithm. Therefore, with this proposed algorithm, the user can benefit from energy efficiency in suitable regions and also confidently use GPR in other regions that are unsuitable for the energy-efficient GPR algorithm.

Acknowledgment

This work was supported by the Scientific Research Projects (BAP) Coordinating Office of Selçuk University.

References

[1] G. Ji, X. Gao, H. Zhang, T.A. Gulliver, "Subsurface object detection using UWB ground penetrating radar", IEEE Pacific Rim Conference on Communications, Computers and Signal Processing, pp. 740-743, 2009.

[2] D.J. Daniels, D.J. Gunton, H.F. Scott, "Introduction to subsurface radar", IEE Proceedings Radar and Signal Processing, Vol. 135, pp. 278-320, 1988.

[3] L.P. Peters Jr, D.J. Daniels, J.D. Young, "Ground penetrating radar as a subsurface environmental sensing tool", Proceedings of the IEEE, Vol. 82, pp. 1802-1822, 1994.

[4] A.J. Alongi, G.G. Clemena, P.D. Cady, Condition Evaluation of Concrete Bridges Relative to Reinforcement Corrosion. Volume 3: Method for Evaluating the Condition of Asphalt-Covered Decks, Washington DC, National Research Council, 1992.

[5] V.M. Malhotra, N.J. Carino, editors, Nondestructive Testing of Concrete, Boca Raton, Florida, CRC Press, 2004.

[6] D. Goodman, "Ground-penetrating radar simulation in engineering and archaeology", Geophysics, Vol. 59, pp. 224-232, 1994.

[7] M.H. Powers, G.R. Olhoeft, "Modeling dispersive ground penetrating radar data", Proceedings of the 5th International Conference on Ground-Penetrating Radar, pp. 173-183, 1994.

[8] K.J. Ellefsen, "Effects of layered sediments on the guided wave in crosswell radar data", Geophysics, Vol. 64, pp. 1698-1707, 1999.

[9] J.M. Carcione, "Ground-penetrating radar: wave theory and numerical simulation in lossy anisotropic media", Geophysics, Vol. 61, pp. 1664-1677, 1996.

[10] F.L. Teixeira, W.C. Chew, M. Straka, M.L. Oristaglio, T. Wang, "Finite-difference time-domain simulation of ground penetrating radar on dispersive, inhomogeneous and conductive soils", IEEE Transactions on Geoscience and Remote Sensing, Vol. 36, pp. 1928-1936, 1998.

[11] K. Holliger, T. Bergman, "Numerical modeling of borehole georadar data", Geophysics, Vol. 67, pp. 1249-1257, 2002.

[12] W.J. Buchanan, N.K. Gupta, "Prediction of electric fields in and around PCBs - 3D finite-difference time-domain approach with parallel processing", Advances in Engineering Software, Vol. 23, pp. 111-114, 1995.

[13] A. Taflove, Computational Electrodynamics: The Finite-Difference Time-Domain Method, Norwood, Massachusetts, Artech House, 1995.

[14] J. Irving, R. Knight, "Numerical modeling of ground-penetrating radar in 2-D using MATLAB", Computers & Geosciences, Vol. 32, pp. 1247-1258, 2006.

[15] W.J. Buchanan, N.K. Gupta, "Parallel processing techniques in EMP propagation using 3D finite-difference time-domain (FDTD) method", Advances in Engineering Software, Vol. 18, pp. 149-159, 1993.

[16] J.P. Berenger, "A perfectly matched layer for the absorption of electromagnetic waves", Journal of Computational Physics, Vol. 114, pp. 185-200, 1994.

[17] S. Ozen, S. Helhel, O.H. Colak, "Electromagnetic field measurements of radio transmitters in urban area and exposure analysis", Microwave & Optical Technology Letters, Vol. 49, pp. 1572-1578, 2007.

[18] L. Seyfi, E. Yaldız, "A novel software for an energy efficient GPR", Advances in Engineering Software, Vol. 41, pp. 1195-1199, 2010.

[19] W.L. Stutzman, G.A. Thiele, Antenna Theory and Design, New York, John Wiley & Sons, 1998.